

The Physics and Cosmology of TeV Blazars

Christoph Pfrommer¹

in collaboration with

Avery E. Broderick², Phil Chang³, Ewald Puchwein¹, Volker Springel¹

¹Heidelberg Institute for Theoretical Studies, Germany

²Perimeter Institute/University of Waterloo, Canada

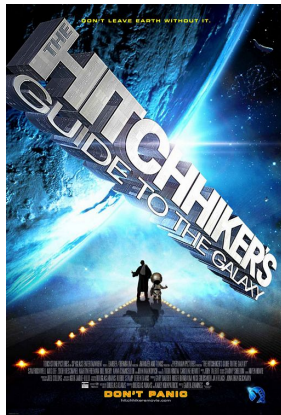
³University of Wisconsin-Milwaukee, USA

Aug 20, 2012 / IAU Beijing



The Hitchhiker's Guide to . . . Blazar Heating

- the extragalactic TeV Universe
- plasma physics of TeV photon propagation
- consequences for
 - **intergalactic magnetic fields**
 - **extragalactic gamma-ray background**
 - **blazar luminosity density**
 - thermal history of the Universe
 - Lyman- α forest
 - formation of dwarf galaxies
 - entropy profile of galaxy clusters

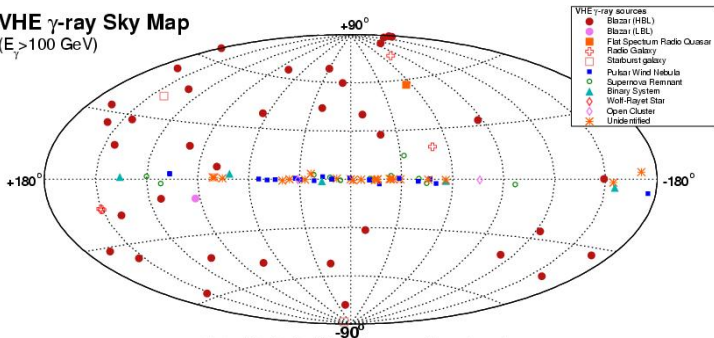


The TeV gamma-ray sky

There are several classes of TeV sources:

- Galactic - pulsars, BH binaries, supernova remnants
- Extragalactic - **mostly** blazars, but how many?

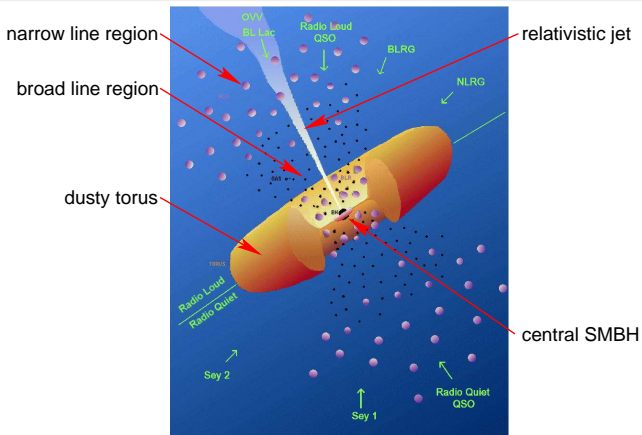
VHE γ -ray Sky Map
($E_\gamma > 100$ GeV)



2011-01-08 - Up-to-date plot available at <http://www.inpp.mpg.de/~rwagner/sources/>

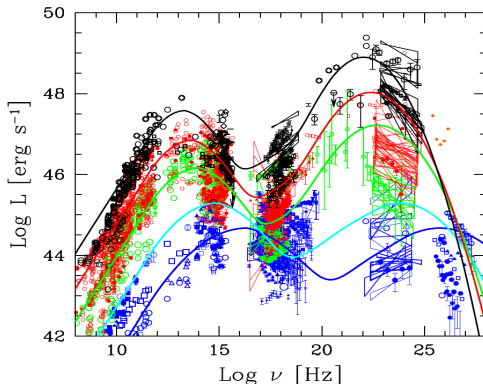


Unified model of active galactic nuclei



→ but blazars and quasars apparently do not share the same cosmological evolution (as otherwise, evolving blazars would overproduce the extragalactic γ -ray background)!

The blazar sequence



Ghisellini (2011), arXiv:1104.0006

- continuous sequence from **LBL**–**IBL**–**HBL**
- TeV blazars are dim (very sub-Eddington)
- TeV blazars have rising spectra in the Fermi band ($\alpha < 2$)
- define TeV blazar = **hard IBL** + **HBL**



Propagation of TeV photons

- 1 TeV photons can pair produce with 1 eV **EBL photons**:

$$\gamma_{\text{TeV}} + \gamma_{\text{eV}} \rightarrow e^+ + e^-$$

- mean free path for this depends on the density of 1 eV photons:
 - $\lambda_{\gamma\gamma} \sim (35 \dots 700)$ Mpc for $z = 1 \dots 0$
 - pairs produced with energy of 0.5 TeV ($\gamma = 10^6$)
- these pairs inverse Compton scatter off the **CMB photons**:
 - mean free path is $\lambda_{\text{IC}} \sim \lambda_{\gamma\gamma}/1000$
 - producing gamma-rays of ~ 1 GeV

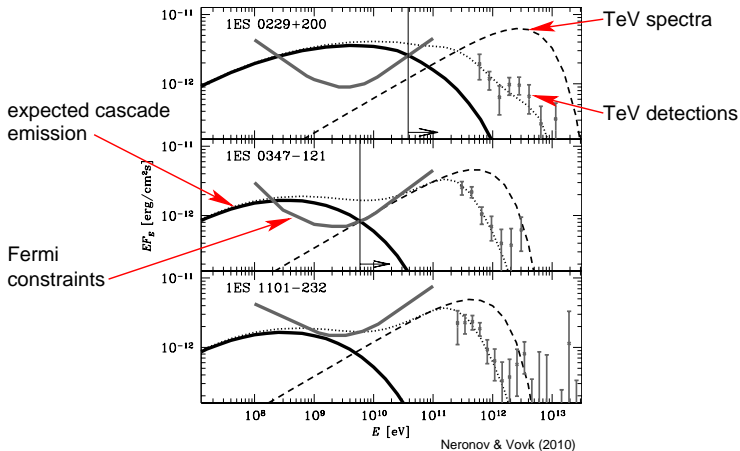
$$E \sim \gamma^2 E_{\text{CMB}} \sim 1 \text{ GeV}$$

- each TeV point source should also be a GeV point source



What about the cascade emission?

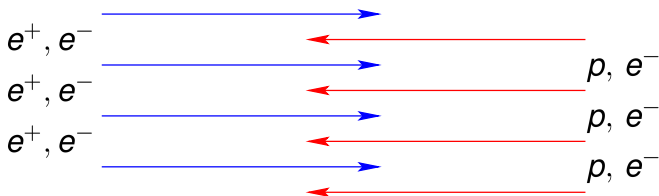
Every TeV source should be associated with a 1-100 GeV gamma-ray halo – **not seen!** → **limits on extragalactic magnetic fields?**



Missing plasma physics?

How do beams of e^+/e^- propagate through the IGM?

- plasma processes are important
- interpenetrating beams of charged particles are unstable
- consider the two-stream instability:



- one frequency (timescale) and one length in the problem:

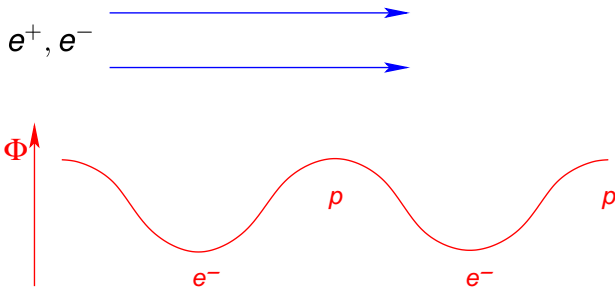
$$\omega_p = \sqrt{\frac{4\pi e^2 n_e}{m_e}}, \quad \lambda_p = \frac{c}{\omega_p} \Big|_{\bar{\rho}(z=0)} \sim 10^8 \text{ cm}$$



Two-stream instability: mechanism

wave-like perturbation with $\mathbf{k} \parallel \mathbf{v}_{\text{beam}}$, longitudinal charge oscillations in background plasma (Langmuir wave):

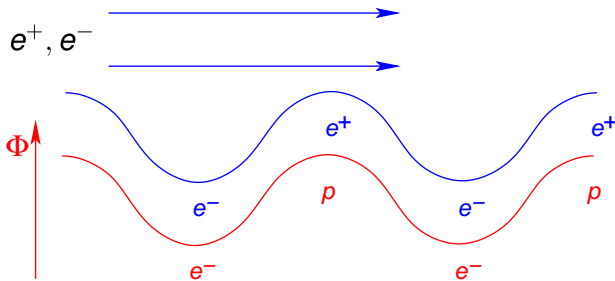
- initially homogeneous beam- e^- :
attractive (repulsive) force by potential maxima (minima)
- e^- attain lowest velocity in potential minima \rightarrow bunching up
- e^+ attain lowest velocity in potential maxima \rightarrow bunching up



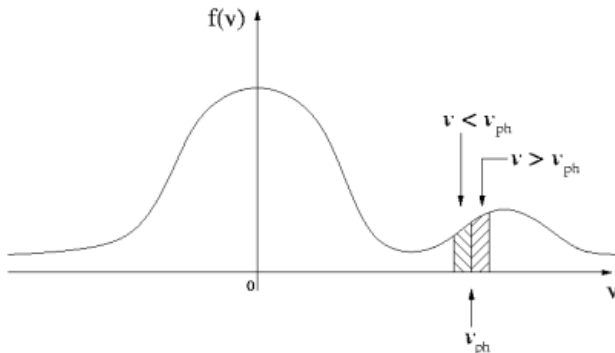
Two-stream instability: mechanism

wave-like perturbation with $\mathbf{k} \parallel \mathbf{v}_{\text{beam}}$, longitudinal charge oscillations in background plasma (Langmuir wave):

- beam- e^+/e^- couple in phase with the background perturbation: enhances background potential
- stronger forces on beam- $e^+/e^- \rightarrow$ positive feedback
- exponential wave-growth \rightarrow instability



Two-stream instability: energy transfer

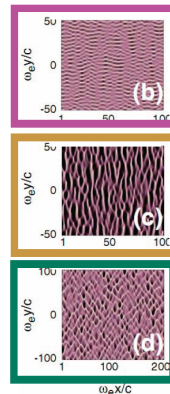
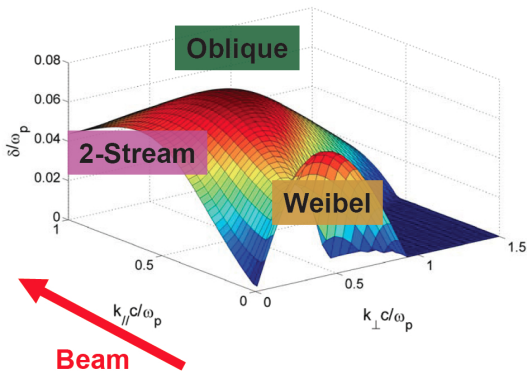


- particles with $v \gtrsim v_{phase}$:
pair energy \rightarrow plasma waves \rightarrow growing modes
- particles with $v \lesssim v_{phase}$:
plasma wave energy \rightarrow pairs \rightarrow damped modes



Oblique instability

k oblique to \mathbf{v}_{beam} : real world perturbations don't choose "easy" alignment = \sum all orientations

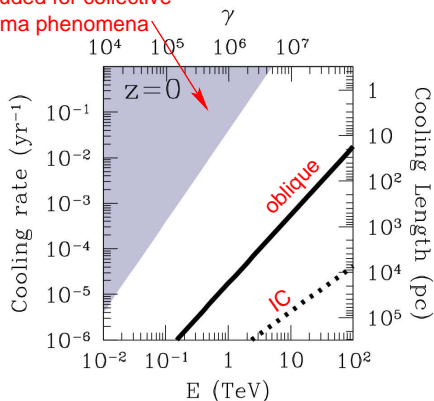


Bret (2009), Bret+ (2010)



Beam physics – growth rates

excluded for collective
plasma phenomena



- consider a light beam penetrating into relatively dense plasma

- maximum growth rate

$$\sim 0.4 \gamma \frac{n_{\text{beam}}}{n_{\text{IGM}}} \omega_p$$

- oblique instability beats IC by two orders of magnitude

Broderick, Chang, C.P. (2012)



Beam physics – complications . . .

non-linear saturation:

- non-linear evolution of these instabilities at these density contrasts is not known
- expectation from PIC simulations suggest substantial isotropization of the beam
- **assume** that they grow at linear rate up to saturation

→ plasma instabilities dissipate the beam's energy, no (little) energy left over for inverse Compton scattering off the CMB



TeV emission from blazars – a new paradigm

$$\gamma_{\text{TeV}} + \gamma_{\text{eV}} \rightarrow e^+ + e^- \rightarrow \begin{cases} \text{IC off CMB} & \rightarrow \gamma_{\text{GeV}} \\ \text{plasma instabilities} & \rightarrow \text{heating IGM} \end{cases}$$

absence of γ_{GeV} 's has significant implications for ...

- intergalactic B -field estimates
- γ -ray emission from blazars: spectra, background

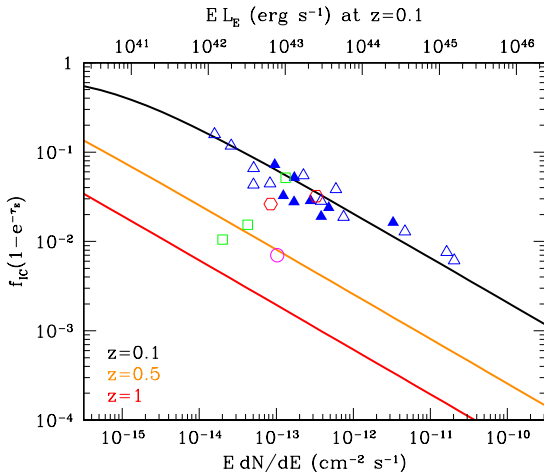
additional IGM heating has significant implications for ...

- thermal history of the IGM: Lyman- α forest
- late time structure formation: dwarfs, galaxy clusters



Implications for B -field measurements

Fraction of the pair energy lost to inverse-Compton on the CMB: $f_{\text{IC}} = \Gamma_{\text{IC}} / (\Gamma_{\text{IC}} + \Gamma_{\text{oblique}})$



Broderick, Chang, C.P. (2012)



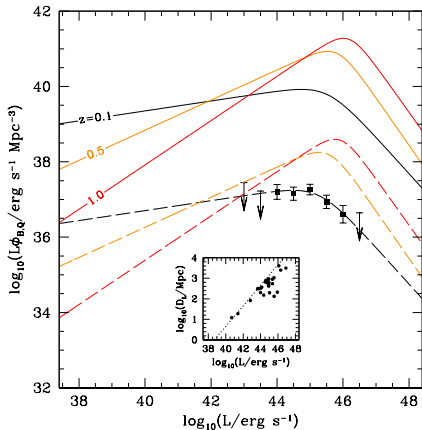
Conclusions on B -field constraints from blazar spectra

- it is thought that TeV blazar spectra might constrain IGM B -fields
- this assumes that cooling mechanism is IC off the CMB + deflection from magnetic fields
- beam instabilities may allow high-energy e^+/e^- pairs to self scatter and/or lose energy
- isotropizes the beam – no need for B -field
- $\lesssim 1\text{--}10\%$ of beam energy to IC CMB photons

→ **TeV blazar spectra are not suitable to measure IGM B -fields (if plasma instabilities saturate close to linear rate)!**



TeV blazar luminosity density: today

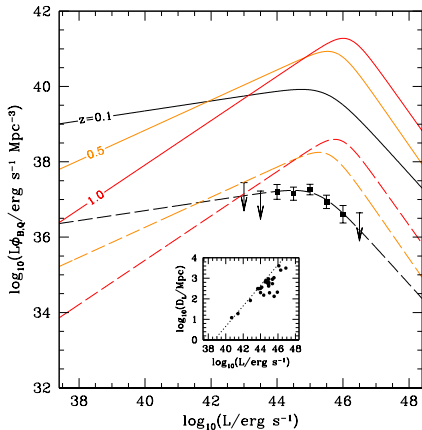


Broderick, Chang, C.P. (2012)

- collect luminosity of all 23 TeV blazars with good spectral measurements
- account for the selection effects (sky coverage, duty cycle, galactic occultation, TeV flux limit)
- TeV blazar luminosity density is a scaled version ($\eta_B \sim 0.2\%$) of that of quasars!



Unified TeV blazar-quasar model



Broderick, Chang, C.P. (2012)

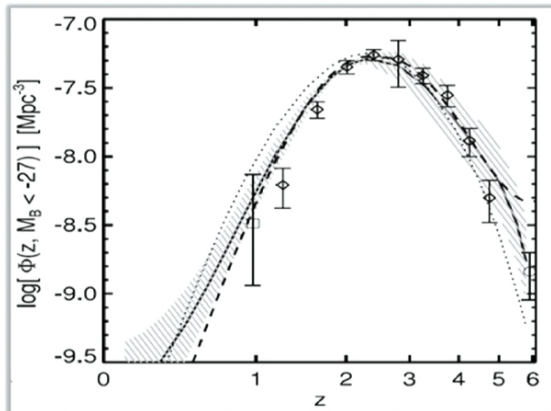
Quasars and TeV blazars are:

- regulated by the same mechanism
- contemporaneous elements of a single AGN population: TeV-blazar activity does not lag quasar activity

→ **assume that they trace each other for all redshifts!**



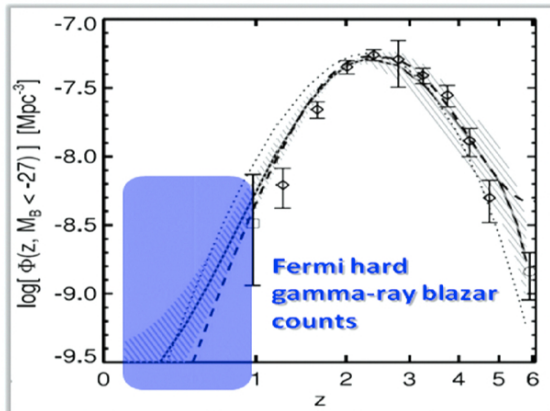
How many TeV blazars are there?



Hopkins+ (2007)



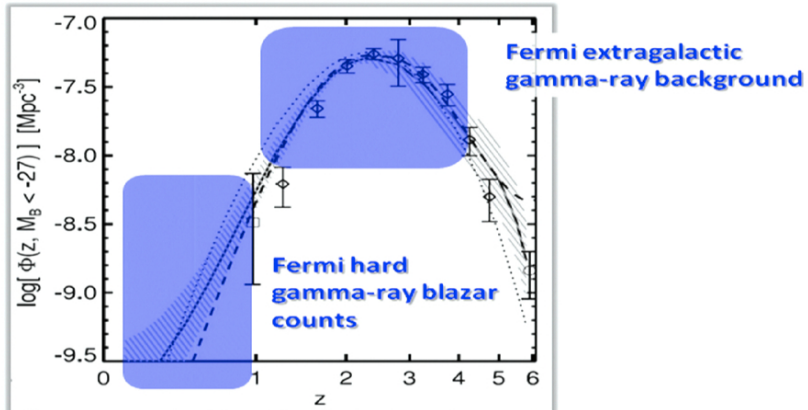
How many TeV blazars are there?



Hopkins+ (2007)



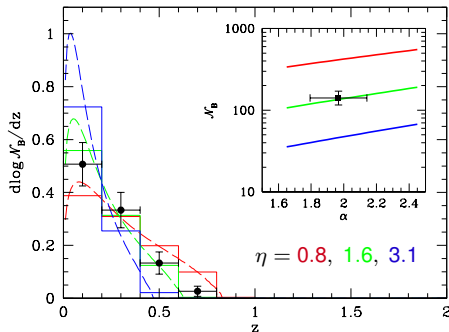
How many TeV blazars are there?



Hopkins+ (2007)



Fermi number count of “TeV blazars”



Broderick, Chang, C.P. (2012)

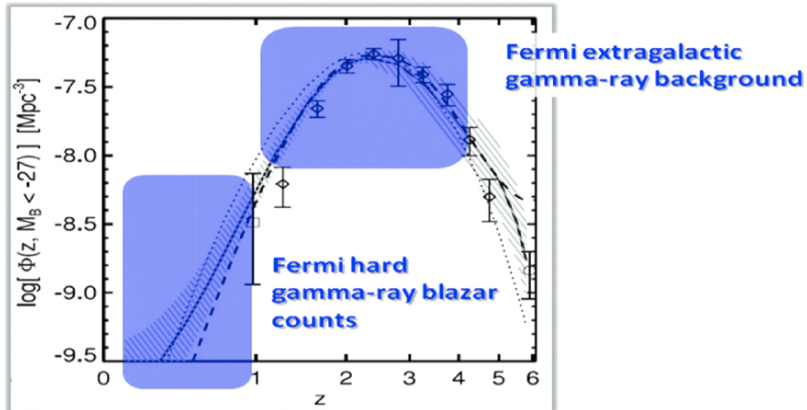
→ **evolving (increasing) blazar population consistent with observed declining evolution (*Fermi* flux limit)!**

- number evolution of TeV blazars that are expected to have been observed by *Fermi* vs. observed evolution
- colors: different flux (luminosity) limits connecting the *Fermi* and the TeV band:

$$L_{\text{TeV},\min}(z) = \eta L_{\text{Fermi},\min}(z)$$



How many TeV blazars are there at high- z ?



Hopkins+ (2007)



Extragalactic gamma-ray background

- assume all TeV blazars have identical intrinsic spectra:

$$F_E = L\hat{F}_E \propto \frac{1}{(E/E_b)^{\alpha_L-1} + (E/E_b)^{\alpha-1}},$$

E_b is break energy,

$\alpha_L < \alpha$ are low and high-energy spectral indexes

- extragalactic gamma-ray background (EGRB):

$$E^2 \frac{dN}{dE}(E, z) = \frac{1}{4\pi} \int_z^\infty dV(z') \frac{\eta_B \tilde{\Lambda}_Q(z') \hat{F}_{E'}}{4\pi D_L^2} e^{-\tau_E(E', z')},$$

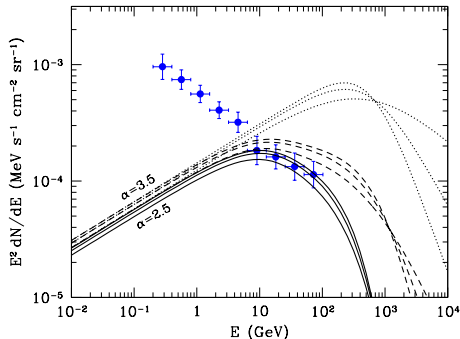
$E' = E(1 + z')$ is gamma-ray energy at *emission*,

$\tilde{\Lambda}_Q$ is physical quasar luminosity density,

$\eta_B \sim 0.2\%$ is blazar fraction, τ is optical depth



Extragalactic gamma-ray background: varying α

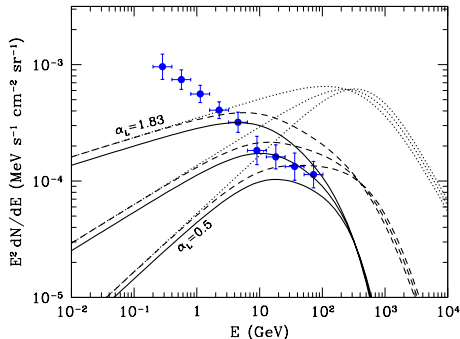


Broderick, Chang, C.P. (2012)

- *dotted*: unabsorbed EGRB due to TeV blazars
- *dashed*: absorbed EGRB due to TeV blazars
- *solid*: absorbed EGRB, after subtracting the resolved TeV blazars ($z < 0.25$)



Extragalactic gamma-ray background: varying α_L

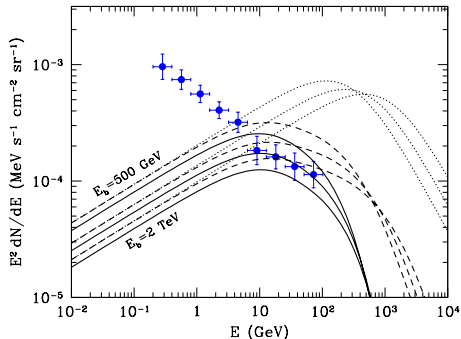


Broderick, Chang, C.P. (2012)

- *dotted*: unabsorbed EGRB due to TeV blazars
- *dashed*: absorbed EGRB due to TeV blazars
- *solid*: absorbed EGRB, after subtracting the resolved TeV blazars ($z < 0.25$)



Extragalactic gamma-ray background: varying E_b



Broderick, Chang, C.P. (2012)

- *dotted*: unabsorbed EGRB due to TeV blazars
- *dashed*: absorbed EGRB due to TeV blazars
- *solid*: absorbed EGRB, after subtracting the resolved TeV blazars ($z < 0.25$)

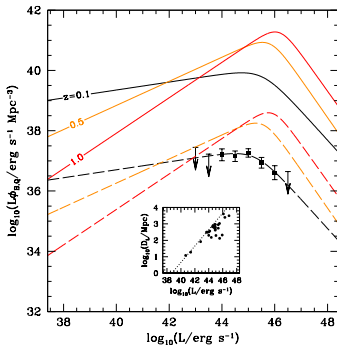


Conclusions on extragalactic gamma-ray background

- the TeV blazar luminosity density is a scaled version of the quasar luminosity density at $z = 0.1$
- assuming that quasars trace TeV blazars for all z and adopting typical spectra, **we can match the *Fermi*-LAT blazar number counts *and* the EGRB!**
- evolving blazars do not overproduce EGRB since the absorbed energy is not reprocessed to GeV energies
- fraction of absorbed energy is greater at higher energies



Prospects for CTA



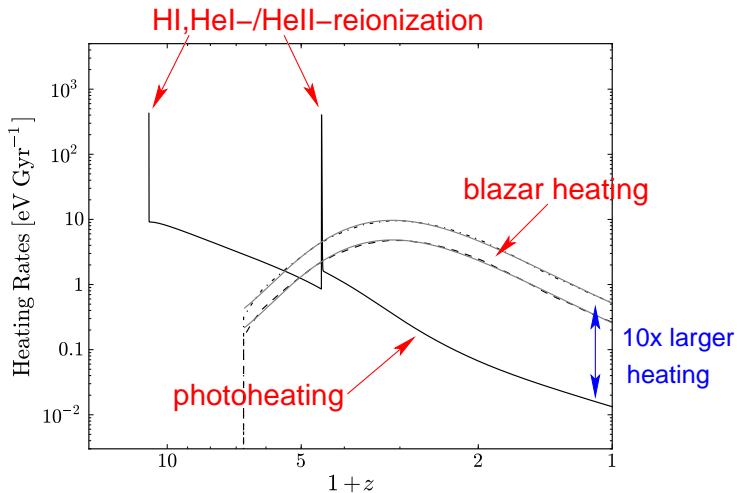
Broderick, Chang, C.P. (2012)

- CTA should find ~ 200 sources above
 $\mathcal{F}_{\min} \simeq 4.2 \times 10^{-12} \text{ erg s}^{-1} \text{ cm}^{-2}$
(our estimate of the effective flux limit of current IACTs)
- if CTA improves \mathcal{F}_{\min} by 5–10, we expect the detection of 1.5×10^3 – 3×10^3 additional TeV blazars, with median luminosities $\sim 3 \times 10^{45} \text{ erg s}^{-1}$

→ more precise estimates for the blazar γ -ray SEDs and a better characterization of their luminosity density, especially at low-luminosities



Evolution of the heating rates



Chang, Broderick, C.P. (2012)



Blazar heating vs. photoheating

- total power from AGN/stars vastly exceeds the TeV power of blazars
- $T_{\text{IGM}} \sim 10^4$ K (1 eV) at mean density ($z \sim 2$)

$$\varepsilon_{\text{th}} = \frac{kT}{m_p c^2} \sim 10^{-9}$$

- radiative energy ratio emitted by BHs in the Universe (Fukugita & Peebles 2004)

$$\varepsilon_{\text{rad}} = \eta \Omega_{\text{bh}} \sim 0.1 \times 10^{-4} \sim 10^{-5}$$

- fraction of the energy energetic enough to ionize H I is ~ 0.1 :

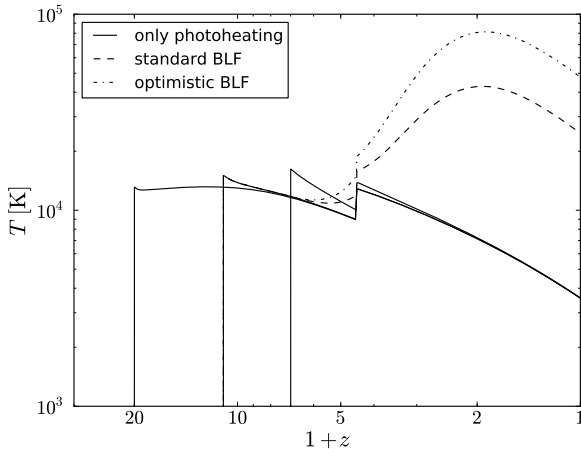
$$\varepsilon_{\text{UV}} \sim 0.1 \varepsilon_{\text{rad}} \sim 10^{-6} \quad \rightarrow \quad kT \sim \text{keV}$$

- photoheating efficiency $\eta_{\text{ph}} \sim 10^{-3} \quad \rightarrow \quad kT \sim \eta_{\text{ph}} \varepsilon_{\text{UV}} m_p c^2 \sim \text{eV}$
 (limited by the abundance of H I/He II due to the small recombination rate)

- blazar heating efficiency $\eta_{\text{bh}} \sim 10^{-3} \quad \rightarrow \quad kT \sim \eta_{\text{bh}} \varepsilon_{\text{rad}} m_p c^2 \sim 10 \text{ eV}$
 (limited by the total power of TeV sources)



Thermal history of the IGM

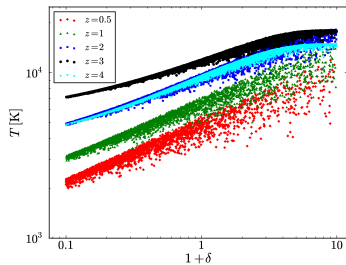


Chang, Broderick, C.P. (2012)

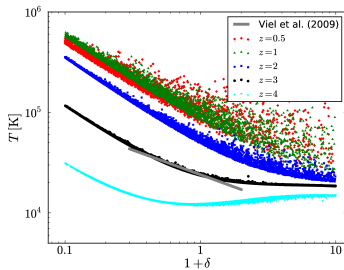


Evolution of the temperature-density relation

no blazar heating



with blazar heating



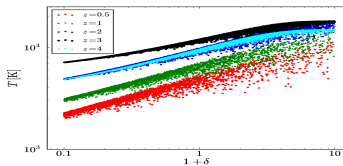
Chang, Broderick, C.P. (2012)

- blazars and extragalactic background light are uniform:
 - blazar heating rate independent of density
 - makes low density regions *hot*
 - causes inverted temperature-density relation, $T \propto 1/\delta$

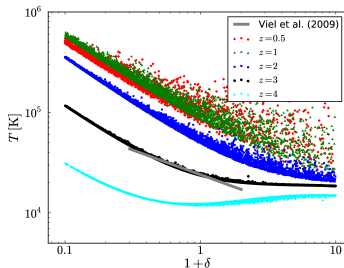


Blazars cause hot voids

no blazar heating



with blazar heating



Chang, Broderick, C.P. (2012)

- blazars completely change the thermal history of the diffuse IGM and late-time structure formation



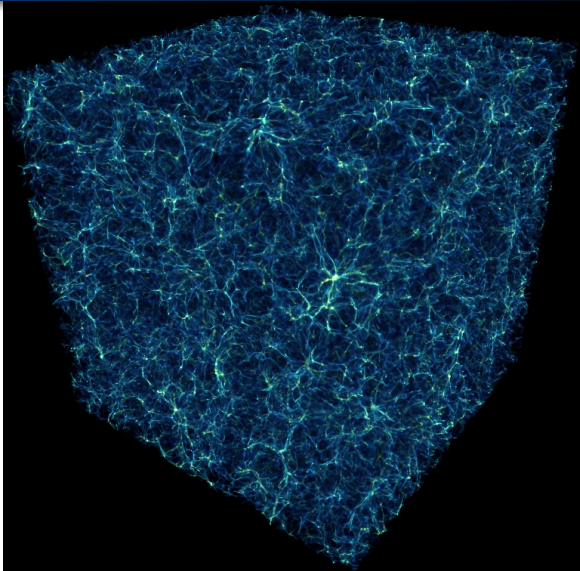
Simulations with blazar heating

Puchwein, C.P., Springel, Broderick, Chang (2012):

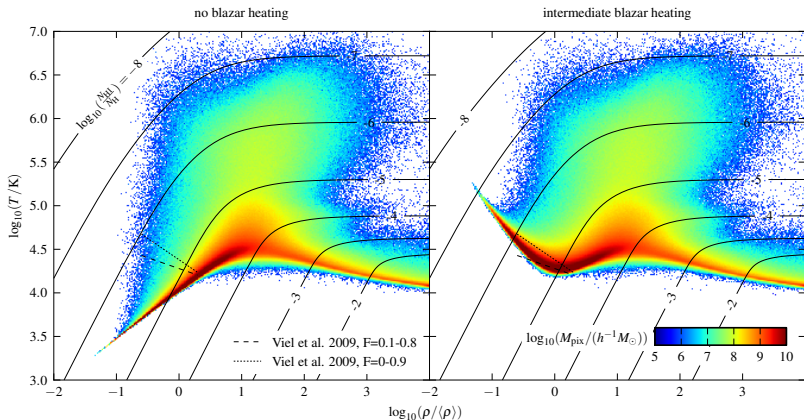
- $L = 15h^{-1}$ Mpc boxes with 2×384^3 particles
- one reference run without blazar heating
- three with blazar heating at different levels of efficiency
(address uncertainty)
- used an up-to-date model of the UV background (Faucher-Giguère+ 2009)



The intergalactic medium



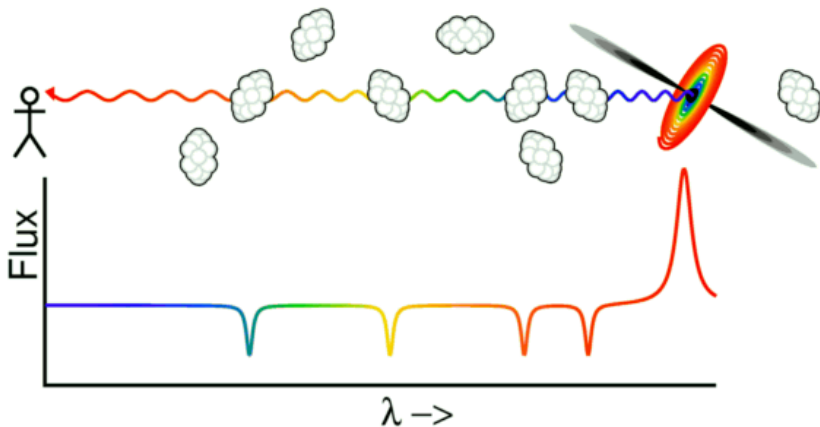
Temperature-density relation



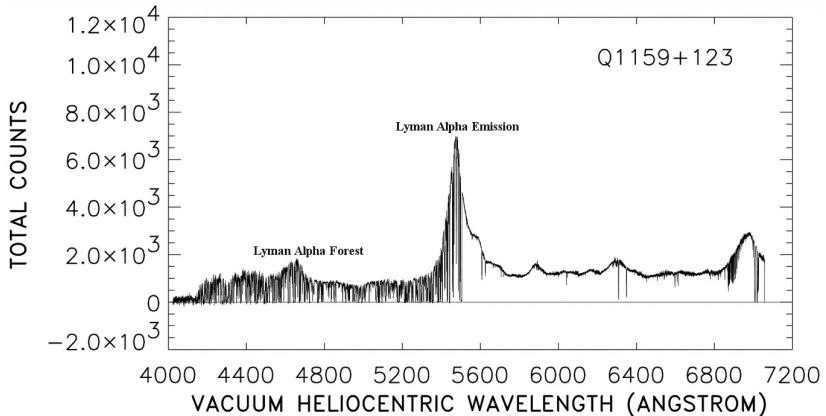
Puchwein, C.P., Springel, Broderick, Chang (2012)



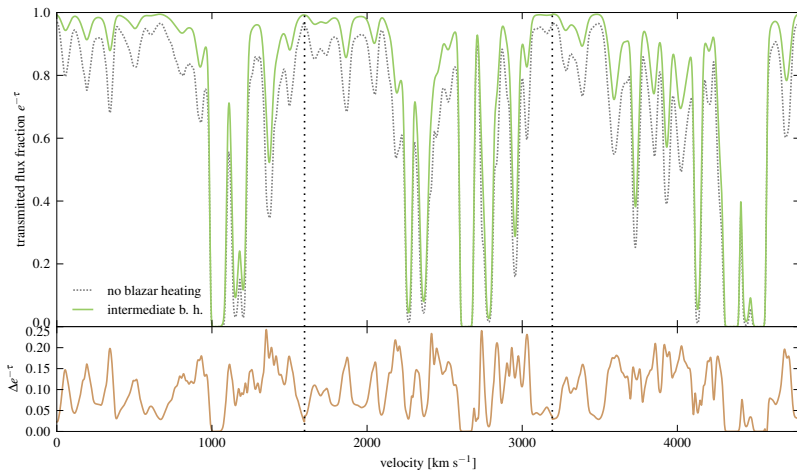
The Lyman- α forest



The observed Lyman- α forest



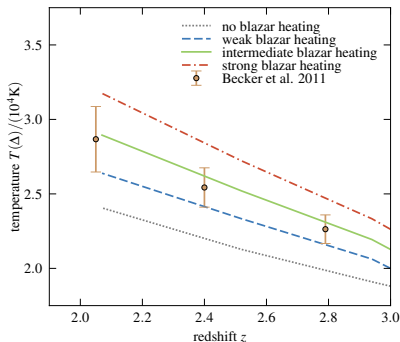
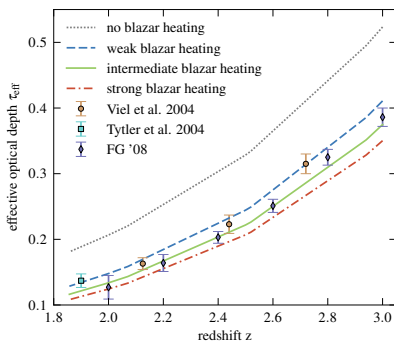
The simulated Ly- α forest



Puchwein+ (2012)



Optical depths and temperatures

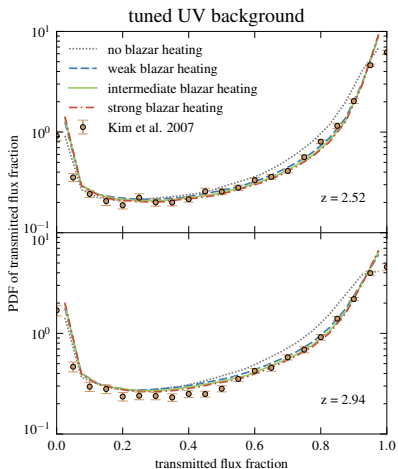


Puchwein+ (2012)

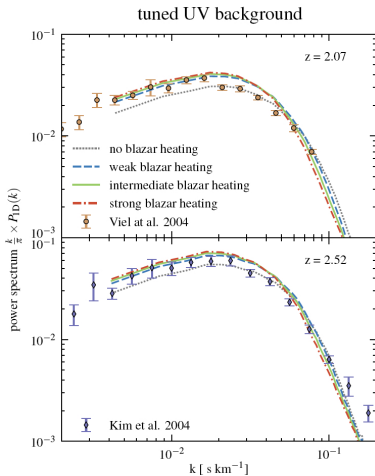
Redshift evolutions of effective optical depth and IGM temperature match data only with additional heating, e.g., provided by blazars!



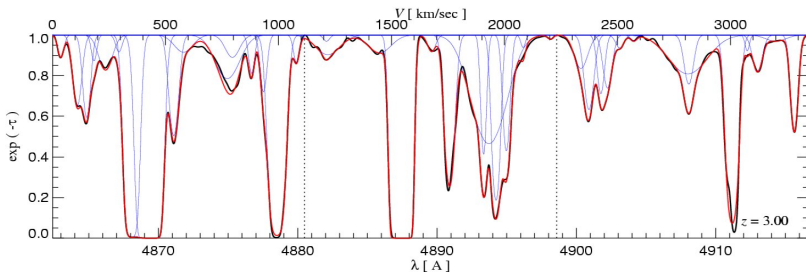
Ly- α flux PDFs and power spectra



Puchwein+ (2012)



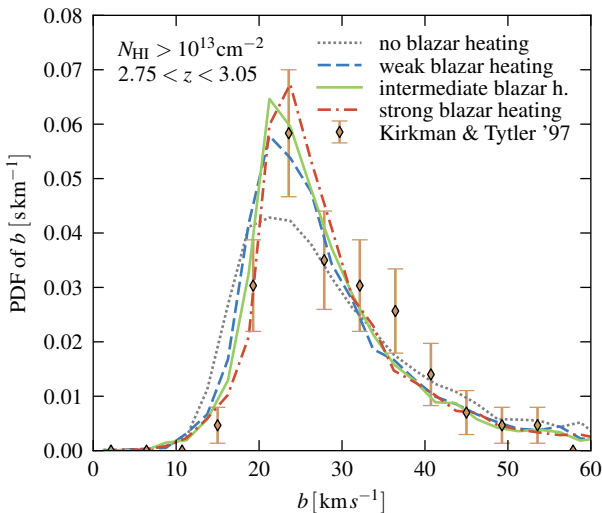
Voigt profile decomposition



- decomposing Lyman- α forest into individual Voigt profiles
- allows studying the thermal broadening of absorption lines



Voigt profile decomposition – line width distribution



Puchwein+ (2012)



Lyman- α forest in a blazar heated Universe

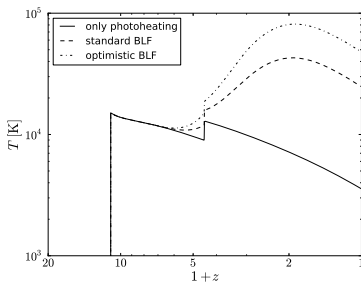
improvement in modelling the Lyman- α forest is a direct consequence of the peculiar properties of blazar heating:

- **heating rate independent of IGM density** \rightarrow naturally produces the inverted $T-\rho$ relation that Lyman- α forest data demand
- **recent and continuous nature of the heating** needed to match the redshift evolutions of all Lyman- α forest statistics
- **magnitude of the heating rate required by Lyman- α forest data** \sim the total energy output of TeV blazars (or equivalently $\sim 0.2\%$ of that of quasars)

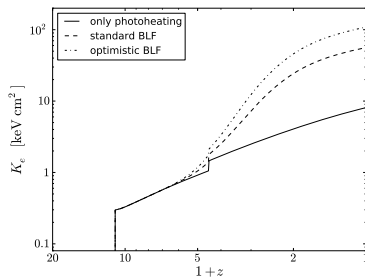


Entropy evolution

temperature evolution



entropy evolution



C.P., Chang, Broderick (2012)

- evolution of entropy, $K_e = kTn_e^{-2/3}$, governs structure formation
- blazar heating: late-time, evolving, modest entropy floor



Dwarf galaxy formation – Jeans mass

- thermal pressure opposes gravitational collapse on small scales
- characteristic length/mass scale below which objects do not form
- hotter IGM \rightarrow higher IGM pressure \rightarrow **higher Jeans mass**:

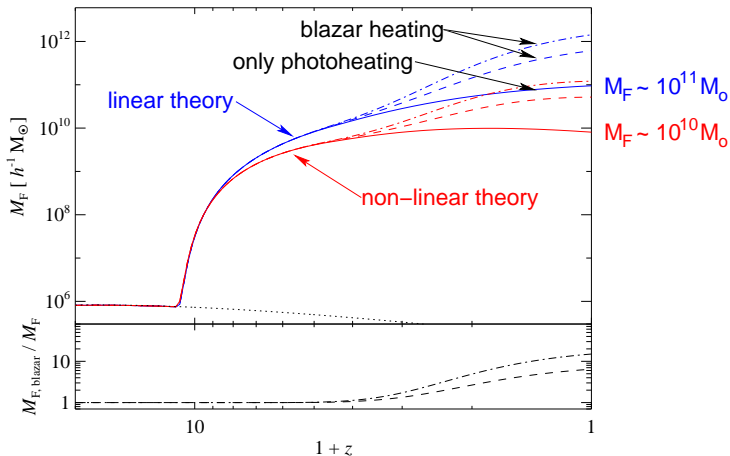
$$M_J \propto \frac{c_s^3}{\rho^{1/2}} \propto \left(\frac{T_{\text{IGM}}^3}{\rho} \right)^{1/2} \rightarrow \frac{M_{J,\text{blazar}}}{M_{J,\text{photo}}} \approx \left(\frac{T_{\text{blazar}}}{T_{\text{photo}}} \right)^{3/2} \gtrsim 30$$

\rightarrow depends on instantaneous value of c_s

- “**filtering mass**” depends on full thermal history of the gas: accounts for delayed response of pressure in counteracting gravitational collapse in the expanding universe
- apply corrections for **non-linear collapse**



Dwarf galaxy formation – Filtering mass

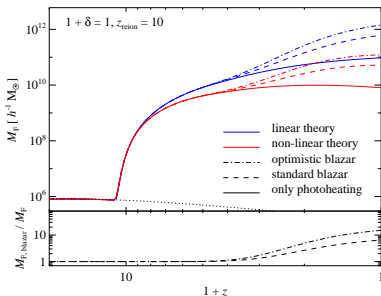


C.P., Chang, Broderick (2012)

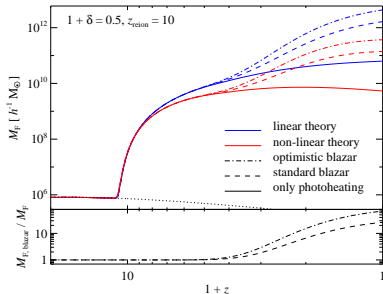


Peebles' void phenomenon explained?

mean density



void, $1 + \delta = 0.5$

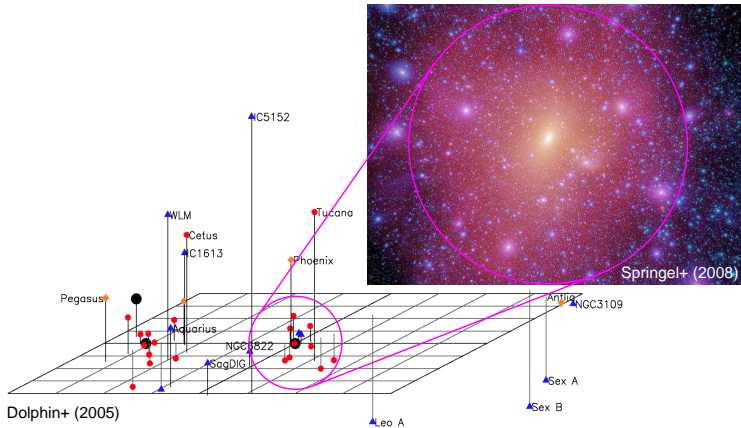


C.P., Chang, Broderick (2012)

- blazar heating efficiently suppresses the formation of void dwarfs within existing DM halos of masses $< 3 \times 10^{11} M_\odot$ ($z = 0$)
- may reconcile the number of void dwarfs in simulations and the paucity of those in observations



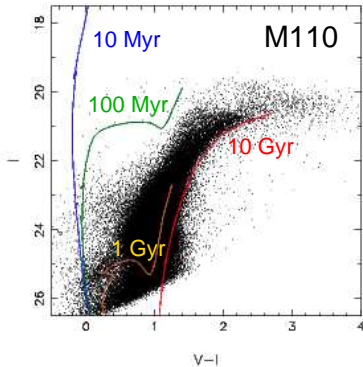
“Missing satellite” problem in the Milky Way



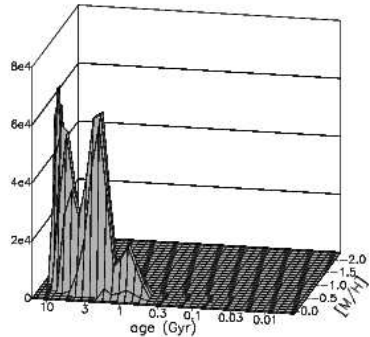
Substructures in cold DM simulations much more numerous than observed number of Milky Way satellites!



When do dwarfs form?



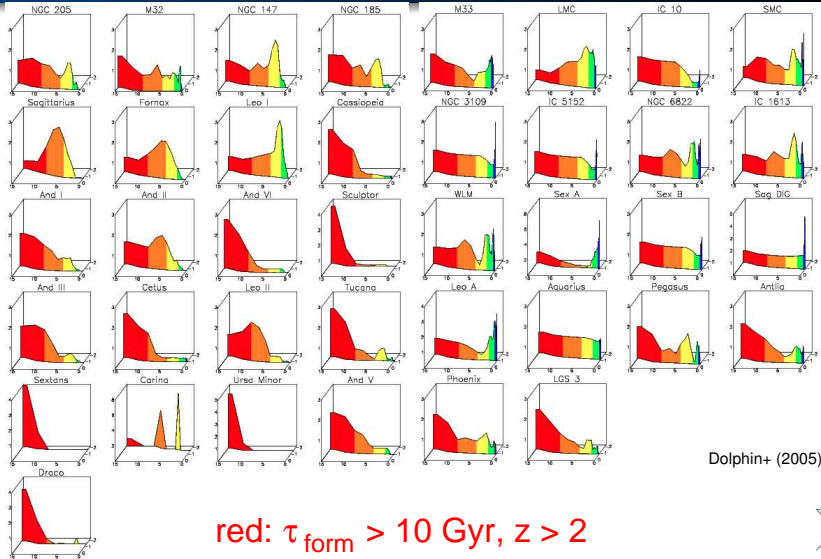
Dolphin+ (2005)



isochrone fitting for different metallicities → star formation histories



When do dwarfs form?

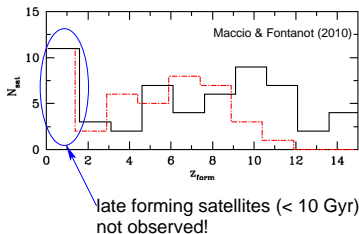


Dolphin+ (2005)

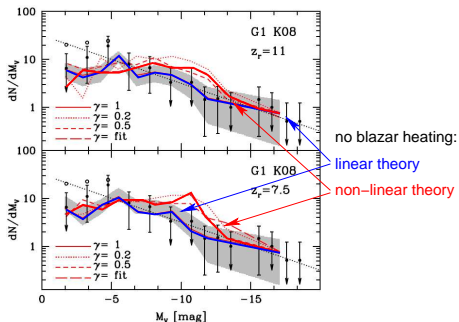


Milky Way satellites: formation history and abundance

satellite formation time



satellite luminosity function



Maccio+ (2010)

- blazar heating suppresses late satellite formation, may reconcile low observed dwarf abundances with CDM simulations

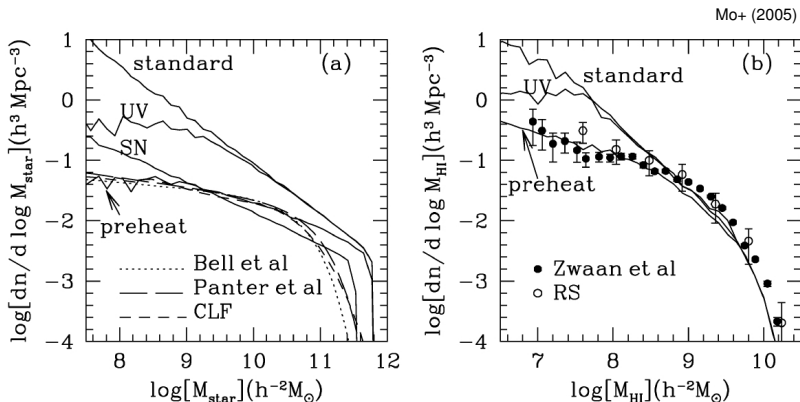


Conclusions on blazar heating

- explains puzzles in high-energy astrophysics:
 - lack of GeV bumps in blazar spectra without IGM B -fields
 - *unified TeV blazar-quasar model* explains Fermi source counts and extragalactic gamma-ray background
- novel mechanism; dramatically alters thermal history of the IGM:
 - uniform and z -dependent preheating
 - rate independent of density \rightarrow inverted $T-\rho$ relation
 - quantitative self-consistent picture of high- z Lyman- α forest
- significantly modifies late-time structure formation:
 - suppresses late dwarf formation (in accordance with SFHs): “missing satellites”, void phenomenon, H I-mass function
 - group/cluster bimodality of core entropy values



Galactic H I-mass function

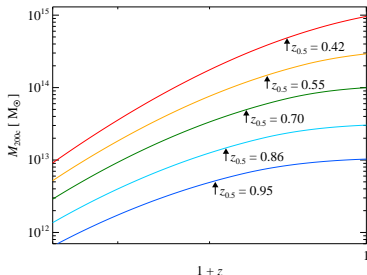


- H I-mass function is too flat (i.e., gas version of missing dwarf problem!)
- photoheating and SN feedback too inefficient
- IGM entropy floor of $K \sim 15 \text{ keV cm}^2$ at $z \sim 2 - 3$ successful!

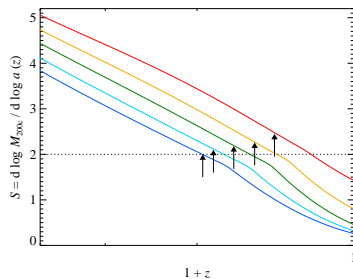


When do clusters form?

mass accretion history



mass accretion rates



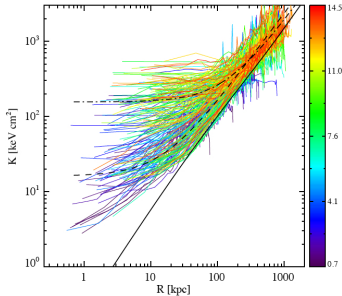
C.P., Chang, Broderick (2012)

- most cluster gas accretes after $z = 1$, when blazar heating can have a large effect (for late forming objects)!



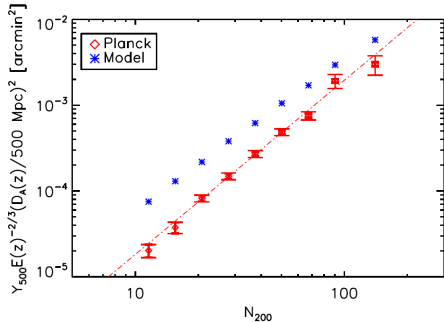
Entropy floor in clusters

Cluster entropy profiles



Cavagnolo+ (2009)

Planck stacking of optical clusters



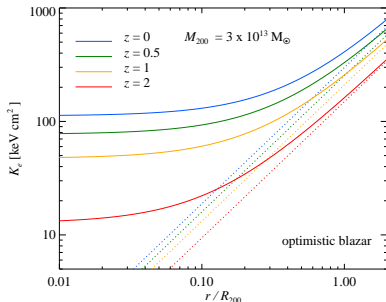
Planck Collaboration (2011)

- Do optical and X-ray/Sunyaev-Zel'dovich cluster observations probe the same population? (Hicks+ 2008, Planck Collaboration 2011)

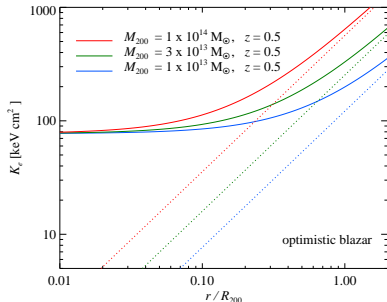


Entropy profiles: effect of blazar heating

varying formation time



varying cluster mass



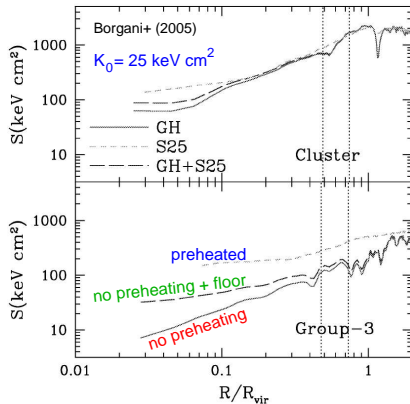
C.P., Chang, Broderick (2012)

assume big fraction of intra-cluster medium collapses from IGM:

- redshift-dependent entropy excess in cores
- greatest effect for late forming groups/small clusters



Gravitational reprocessing of entropy floors

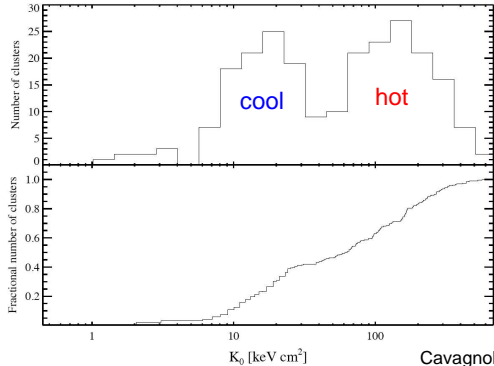


Borgani+ (2005)

- greater initial entropy K_0
 → more shock heating
 → greater increase in K_0
 over entropy floor
- net K_0 amplification of 3-5
- expect:
 median $K_{e,0} \sim 150 \text{ keV cm}^2$
 max. $K_{e,0} \sim 600 \text{ keV cm}^2$

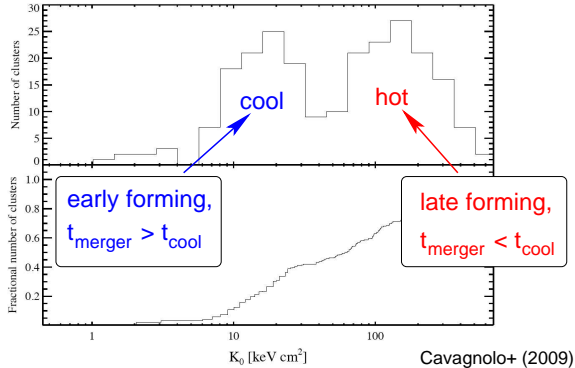


Cool-core versus non-cool core clusters



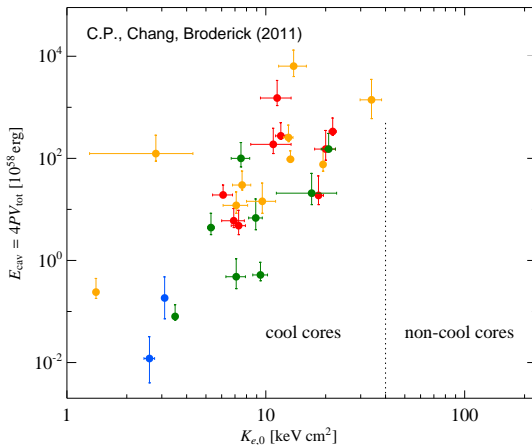
Cavagnolo+ (2009)

Cool-core versus non-cool core clusters

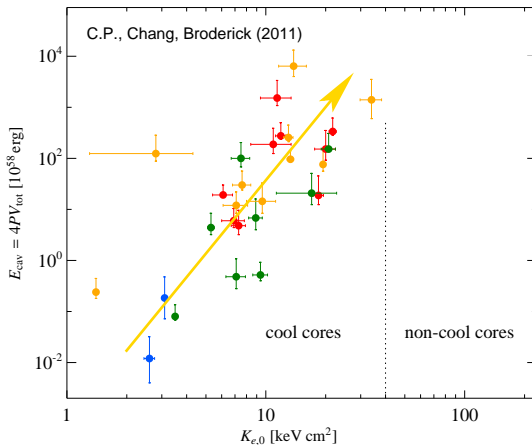


- time-dependent preheating + gravitational reprocessing
→ CC-NCC bifurcation (two attractor solutions)
- need hydrodynamic simulations to confirm this scenario

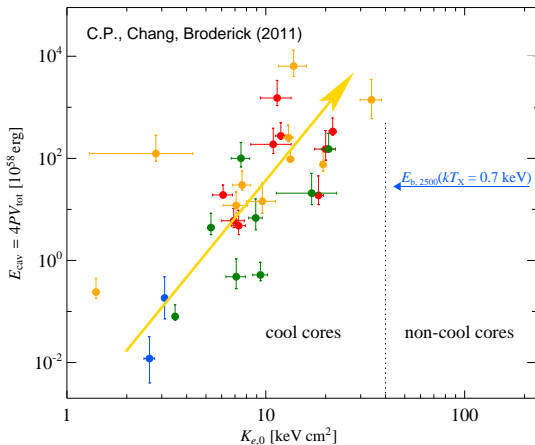
How efficient is heating by AGN feedback?



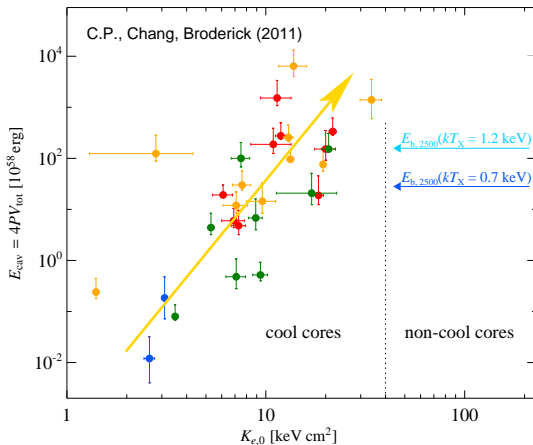
How efficient is heating by AGN feedback?



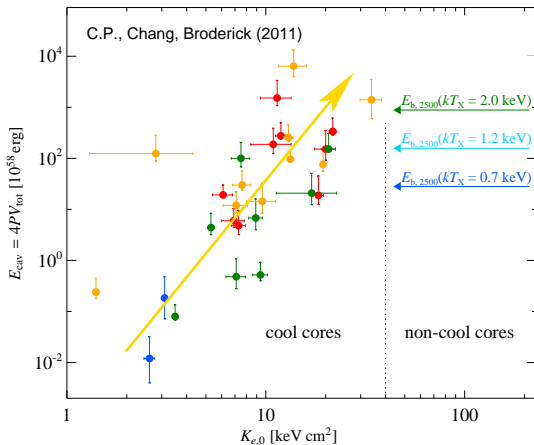
How efficient is heating by AGN feedback?



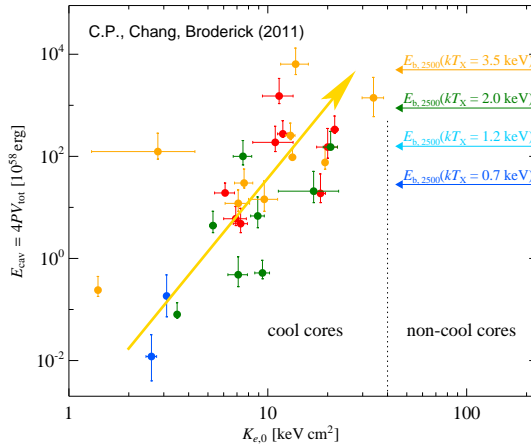
How efficient is heating by AGN feedback?



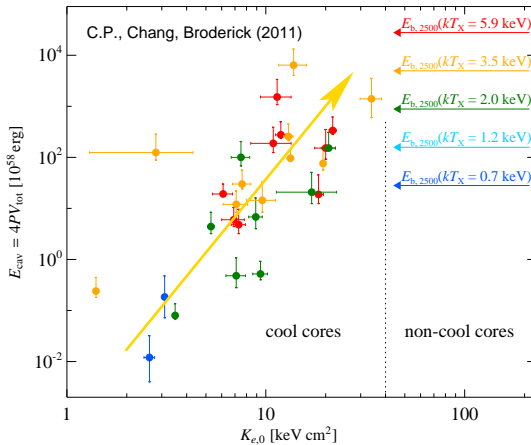
How efficient is heating by AGN feedback?



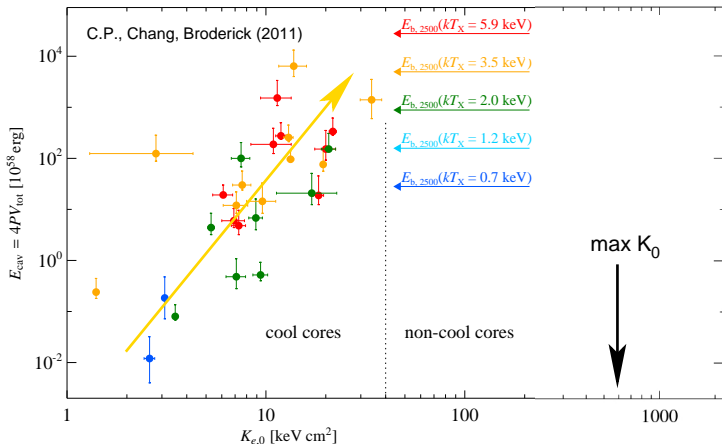
How efficient is heating by AGN feedback?



How efficient is heating by AGN feedback?



How efficient is heating by AGN feedback?



AGNs cannot transform CC to NCC clusters (on a buoyancy timescale)

